Electronic supplementary materials *Mendeleev Commun.*, 2025, **35**, 90–92

Synthesis of MXene/TiO_2 heterostructures for enhanced photocatalytic CO_2 reduction under visible light

Anna Yu. Kurenkova, Danila B. Vasilchenko, Andrey A. Saraev, Roman F. Alekseev, Egor E. Aydakov, Denis D. Mishchenko, Evgeny Yu. Gerasimov and Ekaterina A. Kozlova

Synthesis

Ti_2C_3X MXene ink preparation

The Ti_2C_3 MXene ink were prepared from the Ti_3AlC_2 MAX phase by the etching with LiF/HCl mixture. Specifically, 2.00 g of LiF were dissolved in $4 \cdot 10^{-5}$ m^3 of 7.0 M hydrochloric acid and 2.00 g of Ti_3AlC_2 powder was added in several portions with a constant stirring. The resulting mixture was heated at 45°C for $1.728 \cdot 10^5$ s under constant stirring in polyethylene flask covered with a cap allowing gaseous product to evolve. The resulting suspension was centrifuged and the obtained precipitate was washed several times by centrifugation with water ($4 \cdot 10^{-4}$ m^3 totally) to bring the pH value of the supernatant to about 6-7. The washed precipitate was redispersed in $5 \cdot 10^{-5}$ m^3 of water and resulting suspension was ultrasonicated for 1 h in an ice bath. The as-obtained suspension was centrifuged at 4000 rpm for 300 s and the supernatant was collected and designated as Ti_2C_3 ink. The Ti_2C_3 phase deposited from ink by consecutive deposition-evaporation steps was characterized by PXRD. The UV-Vis spectrum was collected for ink after dilution 20 times by water. The weight percentage of Ti_2C_3 particles in prepared ink (3.7 kg/m^3) was determined gravimetrically after evaporating of weighted portion of ink.

Ti_2C_3X/TiO_2 catalysts preparation

For preparation of 0.5 and 5 wt% of Ti_2C_3X/TiO_2 P25 samples, 425 mg of TiO_2 (Evonik P25) was suspended in $7 \cdot 10^{-6}$ m^3 of water and under constant stirring $6.1 \cdot 10^{-7}$ or $6.1 \cdot 10^{-6}$ m^3 of the Ti_2C_3 ink was added. The resulting suspension was stirred for 24 h at room temperature and then the solid material was separated by filtration on 0.22 μm PTFE porous membrane. The completeness of the deposition was checked by absence of the characteristic absorption band at 800 nm in the UV-Vis spectrum of the supernatant. The collected solid material was washed with water, acetone and dried in an air stream. Finally, the prepared material was dried at 60°C in a vacuum and designated as 0.5 and 5 wt% Ti_2C_3/TiO_2.

Characterization

The photocatalysts that were prepared underwent characterization using X-ray diffraction (XRD), high-resolution transmission electron microscopy (HR TEM), X-ray photoelectron spectroscopy (XPS), UV-vis diffuse reflectance spectroscopy and N_2 low temperature adsorption technique.

XRD patterns were obtained using a Bruker D8 Advance diffractometer (Cu Kα Ni-filtered radiation, λ = 1.5418 Å), which was equipped with a Lynxeye linear detector (Bruker AXS GmbH, Germany). Rietveld refinement was performed for each XRD pattern using GSAS-II software packages.

XPS was performed using an X-ray photoelectron spectrometer (SPECS Surface Nano Analysis GmbH, Germany) equipped with an XR-50 X-ray source with a dual Al/Mg anode and a PHOIBOS-150 hemispherical electron energy analyzer. Core-level spectra were recorded with Al Kα radiation ($h\nu$ = 1486.6 eV). The binding energy calibration was performed by setting C1*s* peak corresponded to titanium carbide at 281.9 eV. Curve fitting was performed with CasaXPS software.[1]

HR TEM images were obtained with a Themis electron microscope (Thermo Fisher Scientific, USA), which operates at a 200 kV accelerating voltage. The microscope boasts a spherical aberration corrector affording a maximum lattice resolution of 0.06 nm and a SuperX energy-dispersive spectrometer (Thermo Fisher Scientific). Ceta 16 CCD sensor (Thermo Fisher Scientific) was employed to capture images.

The diffuse reflectance **UV-vis spectra** were obtained using a Shimadzu UV-2501 PC spectrophotometer with an ISR-240A diffuse reflectance unit. The UV-Vis spectra were recalculated in the Kubelka-Munk coordinates as follows:

$$F(R)=(1-R/100)^{1/2}/(2R/100),$$

where R is the reflectance (%). The optical band gap (E_g) for the synthesized photocatalysts was estimated using the Tauc model for indirect allowed transitions by plotting $(F(R)\times hv)^{1/2}$ versus hv followed by a linear extrapolation to intercept the energy axis.

The textural properties of the samples were measured by **low temperature N_2 adsorption** using an Autosorb-6B instrument (Quantachrome, the United States). The specific surface area was calculated by the Brunauer-Emmett-Teller method.

Photocatalytic tests

The CO_2 reduction reaction was carried out in the batch reactor ($1.7\cdot10^{-4}$ m^3) with quartz window (Fig. S1). The details of the setup for testing the photocatalysts activity are described elsewhere.[2] Ultrapure water ("NuZar Q" water system set) was used for photocatalyst deposition on the glass support and to generate saturated vapor pressure in the reactor. The LED with maximum intensity at 400 nm and power density of 600 W m^{-2} was used as the light source. The gas sample was analyzed with a gas chromatograph "GH-1000" (Chromos, Russia) equipped with NaX and capillary columns; the flame ionization detector and thermal conductivity detector to identify the products of CO_2 reduction and H_2, respectively. Argon was used as carrier gas. Kinetic experiments were carried out for $1.8\cdot10^4$ s (5 h) with hourly gas sampling.

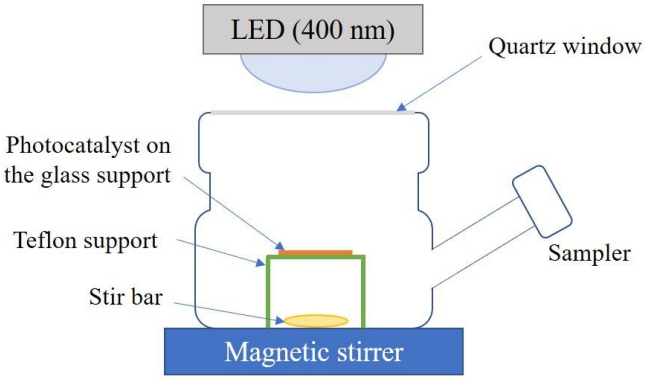

Figure S1. The set-up for photocatalytic CO_2 reduction.

Table S1. Detailed results of XRD analysis for MAX-phase (Ti_3AlC_2) and synthesized MXene (Ti_3C_2).

Phase	Lattice parameters, Å	Weight fraction, %	Crystalline size, nm	d (*002*), Å
MAX-phase (Ti_3AlC_2)				
Ti_3AlC_2 (1) (sp. gr. *$P6_3/mmc$*)	a = 3.0781(2) c = 18.597(1)	67(1)	75(2)	9.30(1)
Ti_3AlC_2 (2) (sp. gr. *$P6_3/mmc$*)	a = 3.0586(4) c = 18.5988(5)	12(1)	370(23)	-
α-Al_2O_3 (sp. gr. *R-3ch*)	a = 4.7584(8) c = 12.990(2)	6(1)	168(20)	-
Al_3Ti (sp. gr. *I4/mmm*)	a = 3.853(1) c = 8.605(3)	15(1)	26(2)	-
MXene (Ti_3C_2)				
Ti_3C_2	-	77(4)	7(1)	9.9(1)
α-Al_2O_3 (sp. gr. *R-3ch*)	a = 4.7588(8) c = 12.989(2)	5(2)	155(40)	-
$TiC_{1-\delta}X_\delta$ (sp. gr. *Fm-3m*)	a = 4.317(2)	18(2)	20(5)	-

Table S2. Textural properties of TiO_2 and Ti_3C_2/TiO_2 photocatalysts. S_{BET} - specific surface area, V – pore volume.

Photocatalyst	**S_{BET}, m^2/g**	**V, cm^3/g**
TiO_2 P25	54	0.20
0.5% Ti_3C_2/TiO_2	49	0.41
5% Ti_3C_2/TiO_2	47	0.42

Table S3. EDX element analysis of Ti_3C_2 (area from Figure 1d).

Z	**Element**	**Atomic %**
6	C	36(5)
22	Ti	33(6)
9	F	17(4)
8	O	13(3)
13	Al	< 1

Table S4. Photocatalytic activities of MXene- and TiO_2-based photocatalysts in gas-phase CO_2 reduction.

№	**Photocatalyst**	**Light source**	**Conditions**	**Product formation rate, μmol g^{-1} h^{-1}**	**v_e, μmol g^{-1} h^{-1}**	**Ref.**
1	1D g-C_3N_4/2D $Ti_3C_2T_x$	300 W Xe-lamp	$NaHCO_3$+ H_2SO_4	CO, 0.73 CH_4, 1.4	13	S3
2	2D/2D/0D $TiO_2/C_3N_4/Ti_3C_2$	350 W Xe-lamp	$NaHCO_3$+ H_2SO_4	CO, 4.39 CH_4, 1.20	18.4	S4
3	Ti_3C_2/g-C_3N_4/ZnO	300 W Xe-lamp	CO_2 (0.02 MPa) + H_2O	CO, 6.41 CH_4, 0.26	14.9	S5
4	g-$C_3N_4/Ti_3C_2T_x$	300 W Xe-lamp	CO_2+H_2O	CO, 3.98 CH_4, 2.12	24.9	S6
5	2D/2D Ti_3C_2 MXene/g-C_3N_4	300 W Xe-lamp, > 420 nm	$NaHCO_3$+ H_2SO_4	CO, 5.19 CH_4, 0.044	10.7	S7
6	g-$C_3N_4/Ti_3C_2T_x/TiO_2$	300 W Xe-lamp	CO_2+H_2O	CO, 8.65 CH_4, 1.23	27.1	S8
7	$ZnIn_2S_4$@TiO_2/Ti_3C_2	150 W Xe-lamp	CO_2+H_2O	CO, 7.5 CH_4, 2.9	38.2	S9
8	Pt/TiO_2 P25	400-nm LED	CO_2+H_2O	CO, 0.08 CH_4, 1.4	11.6	2
9	Ti_3C_2/TiO_2 P25	400-nm LED	CO_2+H_2O	CO, 0.87 CH_4, 2.24	19.7	This study

References

S1. N. Fairley, V. Fernandez, M. Richard-Plouet, C. Guillot-Deudon, J. Walton, E. Smith, D. Flahaut, M. Greiner, M. Biesieger, S. Tougaard, D. Morgan and J. Baltrusaitis, *Appl. Surf. Sci. Adv.*, 2021, **5**, 100112; https://doi.org/10.1016/j.apsadv.2021.100112.

S2. A. A. Saraev, A. Yu. Kurenkova, E. Yu. Gerasimov and E. A. Kozlova, *Nanomaterials*, 2022, **12**, 1584; https://doi.org/10.3 390/nano12091584/S1.

S3. R. Zhong, Y. Liang, F. Huang, S. Liang and S. Liu, *Chin. J. Catal.*, 2023, **53**, 109; https://doi.org/10.1016/S1872- 2067(23)64513-9.

S4. F. He, B. Zhu, B. Cheng, J. Yu, W. Ho and W. Macyk, *Appl. Catal. B*, 2020, **272**, 119006; https://doi.org/10.1016/j.apcatb.2020.119006.

S5. J. Li, Y. Wang, Y. Wang, Y. Guo, S. Zhang, H. Song, X. Li, Q. Gao, W. Shang, S. Hu, H. Zheng and X. Li, *Nano Mater. Sci.*, 2023, **5**, 237; https://doi.org/10.1016/j.nanoms.2023.02.003.

S6. X. Li, Y. Bai, X. Shi, J. Huang, K. Zhang, R. Wang and L. Ye, *Appl. Surf. Sci.*, 2021, **546**, 149111; https://doi.org/10.1016/j.apsusc.2021.149111.

S7. C. Yang, Q. Tan, Q. Li, J. Zhou, J. Fan, B. Li, J. Sun and K. Lv, *Appl. Catal. B*, 2020, **268**, 118738; https://doi.org/10.1016/j.apcatb.2020.118738.

S8. Y. Yang, D. Zhang, J. Fan, Y. Liao and Q. Xiang, *Sol. RRL*, 2021, **5**, 2000351; https://doi.org/10.1002/solr.202000351.

S9. K. C. Devarayapalli, B. Kim, A. R. Manchuri, Y. Lim, G. Kim and D. S. Lee, *Appl. Surf. Sci.*, 2023, **636**, 157865; https://doi.org/10.1016/j.apsusc.2023.157865.